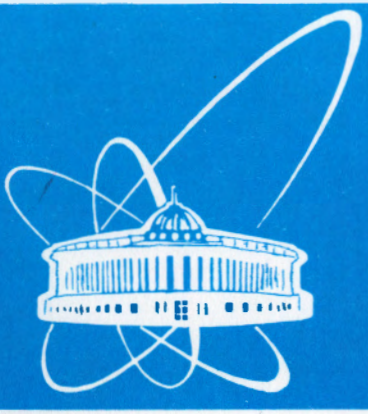

ОБЪЕДИНЕННЫЙ
ИНСТИТУТ
ЯДЕРНЫХ
ИССЛЕДОВАНИЙ

Дубна

E11-99-262

A.G.Abrashkevich[1], M.S.Kaschiev[2], S.I.Vinitsky

A NEW METHOD FOR SOLVING AN EIGENVALUE PROBLEM FOR A SYSTEM OF THREE COULOMB PARTICLES WITHIN THE HYPERSPHERICAL ADIABATIC REPRESENTATION

Submitted to «Journal of Computational Physics»

[1]Chemical Physics Theory Group, Department of Chemistry, University of Toronto, Toronto, ON M5S 3H6, Canada
[2]Institute of Mathematics and Informatics, Bulgarian Academy of Sciences, Sofia 1113, Bulgaria

1999

Абрашкевич А.Г. и др. E11-99-262

Новый метод решения задачи на собственные значения для системы трех кулоновских частиц в гиперсферическом адиабатическом представлении

В рамках адиабатического представления с использованием гиперсферических координат формулируется квантовомеханическая задача трех тел с кулоновским взаимодействием. Сведение многомерной задачи к одномерной осуществляется методом Канторовича. Предложен новый метод для вычисления переменных коэффициентов (потенциальных матричных элементов радиальной связи) результирующей системы обыкновенных дифференциальных уравнений. Метод позволяет вычислять коэффициенты с той же точностью, что и адиабатические функции, полученные как решения вспомогательной параметрической задачи на собственные значения. В предложенном подходе сформулирована новая параметрическая задача относительно неизвестных производных от собственных функций по адиабатической переменной (гиперрадиусу). Предложен быстрый, эффективный и стабильный алгоритм для решения краевой задачи с одинаковой точностью для адиабатических собственных функций и их производных. Развитый метод тестируется на параметрической задаче на собственные значения для атома водорода на трехмерной сфере, которая имеет аналитические решения. Детально исследована точность, эффективность и работоспособность алгоритма. Метод также применен для вычисления энергии основного состояния атома гелия и отрицательного иона водорода.

Работа выполнена в Лаборатории вычислительной техники и автоматизации и Лаборатории теоретической физики им.Н.Н.Боголюбова ОИЯИ.

Препринт Объединенного института ядерных исследований. Дубна, 1999

Abrashkevich A.G. et al. E11-99-262

A New Method for Solving an Eigenvalue Problem for a System of Three Coulomb Particles within the Hyperspherical Adiabatic Representation

The quantum mechanical three-body problem with Coulomb interaction is formulated within the adiabatic represention method using the hyperspherical coordinates. The Kantorovich method of reducing the multi-dimensional problem to the one-dimensional one is used. A new method for computing variable coefficients (potential matrix elements of radial coupling) of a resulting system of ordinary second-order differential equations is proposed. It allows one to calculate the coefficients with the same precision as the adiabatic functions obtained as solutions of an auxiliary parametric eigenvalue problem. In the method proposed, a new boundary parametric problem with respect to unknown derivatives of eigensolutions in the adiabatic variable (hyperradius) is formulated. An efficient, fast and stable algorithm for solving the boundary problem with the same accuracy for the adiabatic eigenfunctions and their derivatives is proposed. The developed method is tested on a parametric eigenvalue problem for a hydrogen atom on a three-dimensional sphere which has an analytical solution. The accuracy, efficiency and robustness of the algorithm are studied in detail. The method is also applied to the computation of the ground state energy of the helium atom and negative hydrogen ion.

The investigation has been performed at the Laboratory of Computing Techniques and Automation and at the Bogoliubov Laboratory of Theoretical Physics, JINR.

Preprint of the Joint Institute for Nuclear Research. Dubna, 1999

1 Introduction

During the last few decades, excitation and ionization processes in a system of three charged particles have been actively studied in atomic and molecular physics [1, 2]. Currently, an ongoing work is carried out at the CERN on experiments ASACUSA and ATHENA studying properties of exotic antiprotonic Coulomb systems in traps at low temperatures using new abilities of modern lasers [3, 4]. These experiments require various data on characteristics of the Coulomb systems, such as helium atom He and antiprotonic helium atom $\bar{p}He^+$, and also on collision processes, leading to the formation of antiprotonic $\bar{p}He^{++}$ and antihydrogen $\overline{H}$ atoms. Detailed calculations of energy levels and widths of metastable states, radiative and Auger transition rates, collision cross sections, etc., are necessary for planning and interpretation of the above experiments. Hence, the development of appropriate numerical methods for computing the desired spectroscopic and collision data with a sufficient accuracy is an important step on the way of better understanding elementary processes taking place in exotic as well as in regular atomic and molecular systems of charged particles.

One of the most popular and widely used approaches for solving the quantum mechanical three-body problem with Coulomb interaction is the adiabatic representation method [1, 2, 5]. In the framework of the hyperspherical coordinates formulation of this method [2, 6, 7], the hyperradius $\mathcal{R}$ is treated as a slowly varying adiabatic variable, analogous to the internuclear distance in the Born-Oppenheimer approximation for molecules [1]. From the mathematical point of view this approach is well known as the Kantorovich method for the reduction of a multi-dimension boundary problem to the one-dimensional one by using a set of solutions of an auxiliary parametric eigenvalue problem [8]. These solutions are obtained for a given set of values of the adiabatic variable, which plays here a role of an external parameter.

This method has been successfully applied for calculating energy levels and wave functions of two-electron atoms within the adiabatic hyperspherical approach (see, e.g., [6, 9]), as well as for computing energy spectra of negative positronium ion Ps^- [7, 10] and various muonic molecules [7, 11] (see also [5, 12]). An essential part in the implementation of the Kantorovich method is the computation of variable coefficients (potential matrix elements) for the final system of the ordinary second-order differential equations. These coefficients are the integrals over eigenfunctions and their derivatives with respect to the

adiabatic variable. In real applications, an efficient and stable computation of derivatives of the adiabatic eigenfunctions and the corresponding integrals with the accuracy comparable with the one achieved for adiabatic eigenfunctions presents a serious challenge for most of the numerical approaches involved in various types of calculations within the adiabatic representation method.

In the present paper we propose a new numerical method for computing these derivatives with the same accuracy as obtained for the eigenvalues and eigenfunctions of the parametric eigenvalue problem. This circumstance guarantees the calculation of the variable coefficients (potential matrix elements of radial coupling) of a system of ordinary differential equations with the same precision as adiabatic eigenfunctions. This goal is achieved by means of formulating a new boundary parametric problem with respect to unknown derivatives of eigenvalues and eigenfunctions in the adiabatic variable. An efficient, fast and stable algorithm for solving this boundary problem with the same precision for the adiabatic eigenfunctions and their derivatives is elaborated.

The accuracy and stability of the method developed are studied on a test parametric problem describing a hydrogen atom on a three-dimensional sphere. This problem has an analytical solution which allows a direct comparison of approximate eigensolutions with the exact ones. To show the efficiency and reliability of our implementation of the Kantorovich method we apply it to the calculation of the ground state energy of the helium atom and negative hydrogen ion. This is a popular problem for three-body Coulomb systems which serves usually as a benchmark for new numerical algorithm and methods. For simplicity, we consider in this paper a system with total angular momentum $J = 0$. This allows us to demonstrate all essential numerical peculiarities of our method when applied to a rather complex atomic system without unnecessary complications connected with accounting for additional angular variables for $J > 0$. The generalization of the present approach for three-body systems with arbitrary total angular momentum is straightforward and will be considered elsewhere.

The paper is organized as follows. The Schrödinger equation for three-dimensional eigenvalue problem for a system of three charged particles is considered in Section 2. The Kantorovich method is briefly described in Section 3. Three steps of implementation of the Kantorovich method are considered in Sections 4-6, respectively. In Section 7 our method is applied to three eigenvalue problems. Numerical solution of a parametric eigenvalue

problem for a hydrogen atom on a three-dimensional sphere is presented in subsection 7.1. The results of our calculations of the ground state energy of the helium atom and negative hydrogen ion are presented in subsection 7.2 where they are compared to the results of other theretical calculations. The conclusions and possible future developments of the method are discussed in Section 8.

2 The Schrödinger equation

Time-independent Schrödinger equation for a system of three charged particles with total angular momentum $J = 0$ in the conventional hyperspherical coordinates $\{\mathcal{R}, \alpha, \theta\}$ [13] can be written as an eigenvalue problem for the following 3-D elliptic equation:

$$\hat{T}\Psi(\mathcal{R},\alpha,\theta) + \frac{1}{\mathcal{R}}\hat{W}(\alpha,\theta)\Psi(\mathcal{R},\alpha,\theta) = \mathcal{E}\Psi(\mathcal{R},\alpha,\theta), \tag{1}$$

where $\mathcal{E}$ is the energy and $\Psi(\mathcal{R},\alpha,\theta)$ is the total wave function of the system. The differential operator $\hat{T}$ and the Coulomb potential $\hat{W}$ are defined in Eq. (1) as follows ($e = \hbar = m_e = 1$):

$$\hat{T} = -\frac{1}{\mathcal{R}^2\tau}\frac{\partial}{\partial\mathcal{R}}\frac{1}{2}\mathcal{R}^2\tau\frac{\partial}{\partial\mathcal{R}} + \hat{t},$$

$$\hat{t} = -\frac{1}{\tau}\left(\frac{\partial}{\partial\alpha}\frac{1}{4}\mathcal{R}\sin^2\alpha\sin\theta\frac{\partial}{\partial\alpha} + \frac{\partial}{\partial\theta}\frac{1}{4}\mathcal{R}\sin\theta\frac{\partial}{\partial\theta}\right),$$

$$\hat{W} = \frac{Z_aZ_c}{\sin\alpha/2} + \frac{Z_bZ_c}{\cos\alpha/2} + Z_aZ_b\left[1 - \sin\alpha\cos\theta\right]^{-1/2},$$

$$\tau = \frac{1}{8}\mathcal{R}^3\sin^2\alpha\sin\theta.$$

In the above, $Z_a = Z_b = -1$ and $Z_c = Z = 2$ $Z_c = Z$ are the charges of particles a, b, and c with masses $M_a = 1$, $M_b = 1$, and $M_c = \infty$, respectively. Note $Z = 1$ for a negative hydrogen ion H^- and $Z = 2$ for a Helium atom He. Hyperradius $\mathcal{R} \in [0,\infty)$, hyperspherical angles $(\alpha,\theta) \in \Omega = \{0 \le \alpha \le \pi,\ 0 \le \theta \le \pi\}$, i.e. total set of variables $(\mathcal{R},\alpha,\theta) \in \Omega_1 = \Omega \times [0,\infty)$.

Total wave function $\Psi(\mathcal{R},\alpha,\theta)$ satisfies the following boundary conditions:

$$\lim_{\alpha\to 0,\pi}\sin^2\alpha\frac{\partial\Psi}{\partial\alpha} = 0, \qquad \lim_{\theta\to 0,\pi}\sin\theta\frac{\partial\Psi}{\partial\theta} = 0, \tag{2}$$

$$\lim_{\mathcal{R}\to 0}\mathcal{R}^5\frac{\partial\Psi}{\partial\mathcal{R}} = 0, \qquad \lim_{\mathcal{R}\to\infty}\mathcal{R}^5\Psi = 0, \tag{3}$$

and is normalized by condition

$$\iiint \mathcal{R}^2 \tau \Psi^2 d\alpha d\theta d\mathcal{R} = 1.$$

3 Kantorovich method

Consider a formal expansion of the solution of Eqs. (1)-(3) over an infinite set of two-dimensional basis functions $\{\Phi_i(\alpha,\theta;\mathcal{R})\}_{i=1}^{\infty}$:

$$\Psi(\mathcal{R},\alpha,\theta) = \sum_{i=1}^{\infty} \chi_i(\mathcal{R})\Phi_i(\alpha,\theta;\mathcal{R}). \tag{4}$$

In Eq. (4) functions $\chi(\mathcal{R})^T = (\chi_1(\mathcal{R}),\chi_2(\mathcal{R}),\ldots)$ are unknown, and adiabatic functions $\Phi(\alpha,\theta;\mathcal{R})^T = (\Phi_1(\alpha,\theta;\mathcal{R}),\Phi_2(\alpha,\theta;\mathcal{R}),\ldots)$ form an orthonormal basis for each value of hyperradius $\mathcal{R}$ which is treated here as a slowly varying adiabatic parameter.

In the Kantorovich approach [8] functions $\Phi_i(\alpha,\theta;\mathcal{R})$ are determined as solutions of the following two-dimensional eigenvalue problem

$$\left(\hat{t} + \frac{1}{\mathcal{R}}\hat{W}\right)\Phi(\alpha,\theta;\mathcal{R}) = \hat{E}(\mathcal{R})\Phi(\alpha,\theta;\mathcal{R}) \tag{5}$$

with boundary conditions derived from Eq. (2):

$$\lim_{\alpha\to 0,\pi} \sin^2\alpha \frac{\partial\Phi}{\partial\alpha} = 0, \qquad \lim_{\theta\to 0,\pi} \sin\theta \frac{\partial\Phi}{\partial\theta} = 0.$$

Since the operator in the left side of Eq. (5) is self-adjoint, its eigenfunctions are orthonormal:

$$\iint \tau\Phi_i\Phi_j d\alpha d\theta = \delta_{ij}.$$

In the equation above, δ_{ij} is Kroneker's δ-symbol. Problem (5) is solved for each value of $\mathcal{R}_k \in \omega_{\mathcal{R}}$ where $\omega_{\mathcal{R}} \doteq (\mathcal{R}_1,\mathcal{R}_2,\ldots,\mathcal{R}_k,\ldots)$ is a given set of values of hyperradius $\mathcal{R}$.

After substitution of expansion (4) in the Rayleigh-Ritz variational functional (see [7])

$$R(\Psi) = \int_{\Omega_1} \mathcal{R}^2 \left\{ \frac{1}{2}\tau\left(\frac{\partial\Psi}{\partial\mathcal{R}}\right)^2 + \frac{\mathcal{R}}{4}\sin\theta\left[\sin^2\alpha\left(\frac{\partial\Psi}{\partial\alpha}\right)^2 + \left(\frac{\partial\Psi}{\partial\theta}\right)^2\right] + \frac{\tau}{\mathcal{R}}\Psi^T\hat{W}\Psi \right\} d\theta d\alpha d\mathcal{R} \times \left\{\int_{\Omega_1} \mathcal{R}^2\Psi^2\tau d\theta d\alpha d\mathcal{R}\right\}^{-1}$$

and subsequent minimization of the functional, the solution of Eqs. (1)-(3) is reduced to a solution of an eigenvalue problem for an infinite set of ordinary second-order differential

equations for determining energy $\mathcal{E}$ and coefficients (radial wave functions) $\chi^T \equiv \chi(\mathcal{R})^T = (\chi_1(\mathcal{R}),\chi_2(\mathcal{R}),\ldots)$ of expansion (4):

$$-\mathbf{I}\frac{1}{\mathcal{R}^2}\frac{d}{d\mathcal{R}}\mathcal{R}^2\frac{d}{d\mathcal{R}}\chi + \mathbf{V}(\mathcal{R})\chi + \mathbf{Q}(\mathcal{R})\frac{d\chi}{d\mathcal{R}} + \frac{1}{\mathcal{R}^2}\frac{d\mathcal{R}^2\mathbf{Q}(\mathcal{R})\chi}{d\mathcal{R}} = 2\mathcal{E}\mathbf{I}\chi, \tag{6}$$

$$\lim_{\mathcal{R}\to 0}\mathcal{R}^2\frac{\partial\chi}{\partial\mathcal{R}} = 0, \qquad \lim_{\mathcal{R}\to\infty}\mathcal{R}^2\chi = 0. \tag{7}$$

Here $\mathbf{I}$, $\mathbf{V}(\mathcal{R})$, and $\mathbf{Q}(\mathcal{R})$ are infinite matrices, elements of which are given by relations

$$\begin{aligned}
&I_{ij} = \delta_{ij}, \quad U_i(\mathcal{R}) = 2E_i(\mathcal{R}) = 2(\hat{E}_i(\mathcal{R}) + \frac{2}{\mathcal{R}^2}),\\
&V_{ij}(\mathcal{R}) = U_i(\mathcal{R})\delta_{ij} - \frac{1}{4\mathcal{R}^2}\delta_{ij} + H_{ij}(\mathcal{R}),\\
&H_{ij}(\mathcal{R}) = H_{ji}(\mathcal{R}) = \iint \tau\frac{\partial\Phi_i}{\partial\mathcal{R}}\frac{\partial\Phi_j}{\partial\mathcal{R}}d\alpha d\theta - \frac{9}{4\mathcal{R}^2}\delta_{ij},\\
&Q_{ij}(\mathcal{R}) = -Q_{ji}(\mathcal{R}) = \iint \tau\Phi_i\frac{\partial\Phi_j}{\partial\mathcal{R}}d\alpha d\theta - \frac{3}{2\mathcal{R}}\delta_{ij}, \quad i,j = 1,2,\ldots.
\end{aligned} \tag{8}$$

Thus, the solution of Sturm-Liouville problem (1)-(3) is reduced to solution of the following three problems:

1. Calculation of potential curves $E_i(\mathcal{R})$ and eigenfunctions $\Phi_i(\alpha,\theta;\mathcal{R})$ of the two-dimensional problem (5)-(2) for a given set of $\mathcal{R} \in \omega_{\mathcal{R}}$.
2. Computation of matrix elements of radial coupling (8) necessary for Eq. (6).
3. Calculation of energies $\mathcal{E}$ and radial wave functions $\chi(\mathcal{R})$ as eigensolutions of one-dimensional eigenvalue problem (6)-(7).

4 Solution of eigenvalue problem (5)

Two-dimensional parametric eigenvalue problem (5)-(2) can be solved directly [7] using the finite element method [14, 15]. In this paper we propose more efficient method of solving this problem. Because of the symmetry of equation coefficients with respect to $\alpha = \pi/2$, problem (5) will be considered for $\alpha \in [0,\pi/2]$.

Consider the following expansion of adiabatic surface function $\Phi_i(\alpha,\theta;\mathcal{R})$:

$$\Phi_i(\alpha,\theta;\mathcal{R}) = \sum_{l=0}^{\infty}\varphi_l^{(i)}(\alpha;\mathcal{R})P_l(\cos\theta), \tag{9}$$

where $\varphi_l^{(i)}(\alpha;\mathcal{R})$ are expansion coefficients depending parametrically on $\mathcal{R}$ and $P_l(\cos\theta)$ are the Legendre polynomials. These polynomials are the eigensolutions of the following eigenvalue problem

$$-\frac{d}{d\theta}\sin\theta\frac{dP_l(\cos\theta)}{d\theta} = \lambda\sin\theta\, P_l(\cos\theta)$$

with $\lambda_l = l(l+1)$ being the corresponding eigenvalues. The Rayleigh-Ritz variational functional for problem (5) can be written as follows

$$R(\Phi) = \int_0^{\pi/2}\cdot\int_0^{\pi}\left[\frac{\mathcal{R}}{4}\sin^2\alpha\sin\theta\left(\frac{\partial\Phi}{\partial\alpha}\right)^2 + \frac{\mathcal{R}}{4}\sin\theta\left(\frac{\partial\Phi}{\partial\theta}\right)^2 + \frac{\mathcal{R}^2}{8}\sin^2\alpha\sin\theta\hat{W}\Phi^2\right]d\theta d\alpha \times \left[\int_0^{\pi/2}\int_0^{\pi}\frac{\mathcal{R}^3}{8}\sin^2\alpha\sin\theta\Phi^2 d\theta d\alpha\right]^{-1} \tag{10}$$

Expansion (9) is substituted next into functional (10). After minimization of the variational functional we get that eigenfunctions $\varphi^T \equiv \varphi_i{}^T \equiv \varphi^{(i)}(\alpha;\mathcal{R})^T = (\varphi_1^{(i)}(\alpha;\mathcal{R}), \varphi_2^{(i)}(\alpha;\mathcal{R}), ...)$ and eigenvalues $E(\mathcal{R}) \equiv E_i(\mathcal{R})$ satisfy the following eigenvalue problem for an infinite set of ordinary differential equations

$$L(\varphi, E) \equiv \left[\mathcal{R}\left(-\frac{d}{d\alpha}\mathbf{D}\frac{d}{d\alpha} + \mathbf{\Lambda}\right) + \mathcal{R}^2\mathbf{W} - E(\mathcal{R})\frac{1}{2}\mathcal{R}^3\mathbf{D}\right]\varphi = 0, \tag{11}$$

$$\lim_{\alpha\to 0,\pi/2}\sin^2\alpha\frac{\partial\varphi}{\partial\alpha} = 0.$$

In the above, $\mathbf{D}$, $\mathbf{\Lambda}$, and $\mathbf{W}$ are infinite matrices elements of which are defined by

$$D_{ll} = \frac{1}{4}\sin^2\alpha, \quad D_{ll'} = 0,\ l \neq l', \quad \Lambda_{ll} = \frac{1}{4}\left(l(l+1) + \sin^2\alpha\right), \quad \Lambda_{ll'} = 0,\ l \neq l',$$

$$W_{ll'} = \int_0^{\pi} P_l(t)\hat{W}(\alpha,\theta)P_{l'}(t)\tau d\theta = -Z\frac{1}{4}\sin\alpha\left(\cos\frac{\alpha}{2} + \sin\frac{\alpha}{2}\right)\delta_{ll'} + \frac{1}{8}\sin^2\alpha W_{ll'}^{rep},$$

$$W_{ll'}^{rep} = \int_{-1}^{1}\frac{P_l(t)P_{l'}(t)}{\sqrt{1-t\sin\alpha}}dt, \quad t = \cos\theta, \quad l, l' = 0, 1, 2, \ldots.$$

Thus, the solution of the two-dimensional eigenvalue problem (5)-(2) is reduced to the solution of eigenvalue problem (11) for a system of the ordinary second-order differential equations. Note that to write eq.(11) we add term $2/\mathcal{R}^2$ to Hamiltonian (5) to calculate instead of the original eigenvalue $\hat{E}_i(\mathcal{R})$ the shifted eigenvalue $E(\mathcal{R}) = \hat{E}(\mathcal{R}) + 2/\mathcal{R}^2$ which has been introduced previously in definition (8) and corresponded to eigenvalue of the conventional parametric eigenvalue problem [21].

5 Solution of eigenvalue problems (6) and (11)

For numerical solution of one-dimensional eigenvalue problems (6) and (11) subject to the corresponding boundary conditions, the high order approximations of the finite element method [14, 15] elaborated in our previous papers [16, 17] have been used. One-dimensional finite elements of order $p = 1, 2, \ldots, 10$ have been implemented. Using the standard finite element procedures [15], problems (6) and (11) are approximated by the generalized algebraic eigenvalue problem

$$\mathbf{A}\mathbf{F}^h = E^h\mathbf{B}\mathbf{F}^h, \tag{12}$$

where $\mathbf{A}$ is the stiffness matrix, $\mathbf{B}$ is the mass matrix, E^h is the corresponding eigenvalue, and $\mathbf{F}^h$ is the vector approximating solutions of (6) or (11) on the finite-element grid. For problem (6), $\mathbf{A} = \tilde{\mathbf{K}}_1 + \tilde{\mathbf{K}}_2 + \tilde{\mathbf{K}}_3$ and $\mathbf{B} = \tilde{\mathbf{M}}$, where matrices $\tilde{\mathbf{K}}_1$, $\tilde{\mathbf{K}}_2$ and $\tilde{\mathbf{K}}_3$ correspond to the first, the second, and the third and fourth terms in the left hand side of Eq. (6), respectively, and matrix $\tilde{\mathbf{M}}$ corresponds to the term in the right hand side of Eq. (6). For problem (11), $\mathbf{A} = \mathcal{R}\mathbf{K}_1 + \mathcal{R}^2\mathbf{K}_2$ and $\mathbf{B} = \mathcal{R}^3\mathbf{M}$, where matrices $\mathbf{K}_1, \mathbf{K}_2$, and $\mathbf{M}$ correspond to the first, the second, and the third terms in Eq. (11), respectively. The $\mathbf{A}$ and $\mathbf{B}$ matrices are symmetric and have a banded structure, and $\mathbf{B}$ matrix is also positive defined. The algebraic eigenvalue problem (12) is solved using the subspace iteration method [15].

Let E_n, φ_n are the exact solution of (11) and $E_n^h, \mathbf{F}_n^h$ are the numerical solution of (12). Then the following estimates are valid [14]

$$|E_n - E_n^h| \leq c_1(E_n)h^{2p}, \quad ||\varphi_n - \mathbf{F}_n^h||_0 \leq c_2(E_n)h^{p+1}, \quad c_1 > 0, \quad c_2 > 0, \tag{13}$$

where h is the grid step, p is the order of finite elements, n is the number of the corresponding eigensolution, and constants c_1 and c_2 do not depend on step h. The same estimates are valid for the approximate solutions of problem (6).

6 Calculations of matrix elements of radial coupling

Calculation of potential matrices $\mathbf{V}(\mathcal{R})$ and $\mathbf{Q}(\mathcal{R})$ (see Eq. (8)) with sufficiently high accuracy is a very important step of solving a system of radial equations (6), since otherwise it is practically impossible to get the desired energies and wave functions of three-body Coulomb systems with required precision. This implies that derivatives $\frac{d\varphi}{d\mathcal{R}}$ should be

computed with the highest possible accuracy, which presents a difficult problem for most of numerical methods usually used in the adiabatic representation calculations. In the most of applications the following formulas

$$Q_{ij}(\mathcal{R}) = [\mathcal{R}(E_i(\mathcal{R}) - E_j(\mathcal{R}))]^{-1} \int_0^{\pi/2} \varphi_i^T \mathcal{R}^2 \mathbf{W} \varphi_j d\alpha \tag{14}$$

and

$$H_{ij}(\mathcal{R}) = -\sum_l Q_{il}(\mathcal{R}) Q_{lj}(\mathcal{R}), \quad Q_{ii}(\mathcal{R}) = 0, \tag{15}$$

are usually used. Note that Eq. (15) has a rather slow convergence which means that in order to get a high level of accuracy one should include a sufficiently large number of terms in a sum over l. This circumstance can present a serious problem from the computational point of view; especially in regard to demands for required computational resources and computation time.

The main goal of this paper is to develop an effective numerical method that will allow one to calculate derivative $\frac{d\varphi}{d\mathcal{R}}$ with the same accuracy as achieved for eigenfunctions of (11) and to use it to compute matrix elements defined by formulas (8). Taking a derivative of (11) with respect to $\mathcal{R}$, we get that $\frac{d\varphi}{d\mathcal{R}}$ can be obtained as a solution of the following boundary problem

$$L\left(\frac{d\varphi}{d\mathcal{R}}, E\right) = \left[\frac{d}{d\alpha}\mathbf{D}\frac{d}{d\alpha} - \mathbf{\Lambda} - 2\mathcal{R}\mathbf{W} + \frac{3}{2}E(\mathcal{R})\mathcal{R}^2\mathbf{D} + \frac{1}{2}E'(\mathcal{R})\mathcal{R}^3\mathbf{D}\right]\varphi \equiv G. \tag{16}$$

The boundary conditions for function $\frac{d\varphi}{d\mathcal{R}}$ are the same as for function φ. Taking into account that $E(\mathcal{R})$ is an eigenvalue of operator L, problem (16) will have a solution *if and only if the right hand side term G is orthogonal to the eigenfunction φ*. From this condition we find that

$$E'(\mathcal{R}) = \int_0^{\pi/2} \left[\frac{d\varphi}{d\alpha}^T \mathbf{D}\frac{d\varphi}{d\alpha} + \varphi^T(\mathbf{\Lambda} + 2\mathcal{R}\mathbf{W})\varphi\right] d\alpha - \frac{3}{\mathcal{R}}E(\mathcal{R}). \tag{17}$$

Now the problem (16) has a solution, but it is not unique. From the normalization condition

$$\int_0^{\pi/2} \varphi^T \frac{1}{2}\mathcal{R}^3 \mathbf{D}\varphi d\alpha = 1$$

we obtain the required additional condition

$$\int_0^{\pi/2} \varphi^T \frac{1}{2}\mathcal{R}^3 \mathbf{D}\frac{d\varphi}{d\mathcal{R}} d\alpha = -\frac{3}{2\mathcal{R}}. \tag{18}$$

Thus, problem (16) with additional conditions (17)-(18) has now a unique solution. It is necessary to mention that the second estimate of Eq. (13) is valid also for solution $\frac{d\varphi}{d\mathcal{R}}$ of problem (16)-(18). This fact guarantees the same accuracy for adiabatic functions and their derivatives within the present method.

Let us consider a numerical algorithm for the computation of derivative $\frac{d\varphi}{d\mathcal{R}}$. It follows from Eq. (12) that we should solve the following linear system of algebraic equations

$$\mathbf{K}\mathbf{u} \equiv (\mathbf{A} - E^h\mathbf{B})\mathbf{u} = \mathbf{b}, \quad \mathbf{u} = \frac{d\mathbf{F}^h}{d\mathcal{R}}, \tag{19}$$

where

$$\mathbf{A} = \mathcal{R}\mathbf{K_1} + \mathcal{R}^2\mathbf{K_2}, \quad \mathbf{B} = \mathcal{R}^3\mathbf{M},$$

$$\mathbf{b} = [-\mathbf{K_1} - 2\mathcal{R}\mathbf{K_2} + (3E^h + \mathcal{R}(E^h)')\mathcal{R}^2\mathbf{M}]\mathbf{F}^h,$$

$$(E^h)' = (\mathbf{F}^h)^T[\mathbf{K_1} + 2\mathcal{R}\mathbf{K_2}]\mathbf{F}^h - \frac{3}{\mathcal{R}}E^h.$$

In these expressions $\mathbf{K_1}$, $\mathbf{K_2}$ and $\mathbf{M}$ are the finite element matrixes which corresponded to the first, second and third terms in equation (11) with $\mathcal{R} = 1$. Since E^h is an eigenvalue of (12), matrix $\mathbf{K}$ in Eq. (19) is degenerate. The algorithm for solving Eq. (19) can be written in three steps as follows:

Step 1. The additional condition (18) has the form

$$\mathbf{u}^T\mathbf{B}\mathbf{F}^h = -\frac{3}{2\mathcal{R}}.$$

Denote by k a number determined by the condition

$$|\mathbf{B}\mathbf{F}^h|_k = \max_{1\le i\le N} |\mathbf{B}\mathbf{F}^h|_i, \quad C_k = (\mathbf{B}\mathbf{F}^h)_k,$$

where N is the order of matrices above.

Step 2. Solve two systems of algebraic equations

$$\overline{\mathbf{K}}\overline{v} = \overline{\mathbf{b}}, \quad \overline{\mathbf{K}}\overline{w} = \mathbf{c},$$

where

$$\mathbf{c}^T = (K_{1k}, K_{2k}, \ldots, K_{Nk}), \quad c_k = 0, \quad \overline{b}_i = b_i, \quad \overline{b}_k = 0,$$

$$\overline{\mathbf{K}}_{ij} = \mathbf{K}_{ij}, \quad i \neq k, \quad j \neq k, \quad \overline{\mathbf{K}}_{ik} = 0, \quad i \neq k, \quad \overline{\mathbf{K}}_{kj} = 0, \quad j \neq k, \quad \overline{\mathbf{K}}_{kk} = 1.$$

In this way we have $\overline{v}_k = 0$ and $\overline{w}_k = 0$.

Step 3. Find constants γ, γ_1 and γ_2 as

$$\gamma_1 = \overline{\mathbf{v}}^T \mathbf{B} \mathbf{F}^h, \quad \gamma_2 = \overline{\mathbf{w}}^T \mathbf{B} \mathbf{F}^h, \quad \gamma = -\frac{3 + 2\mathcal{R}\gamma_1}{2\mathcal{R}(C_k - \gamma_2)}.$$

After that derivative $\mathbf{u} = \dfrac{d\mathbf{F}^h}{d\mathcal{R}}$ is obtained using formula

$$u_i = \overline{v}_i - \gamma \overline{w}_i, \quad i \neq k, \quad u_k = \gamma.$$

From the consideration above it is evident, that the derivative computed has the same accuracy as the calculated eigenfunction.

7 Numerical results

In this Section we apply our approach to three problems which allow us to demonstrate high accuracy, efficiency and stability of the algorithm developed. The first test problem solves the eigenvalue problem for a hydrogen atom on a three-dimensional sphere. This problem has an analytical solution which allows a direct comparison of approximate eigensolutions obtained by our method to the exact solutions. The other two problems are devoted to the computation of the ground state energy of the helium atom and negative hydrogen ion, respectively. Such eigenvalue problem is usually used as a benchmark for testing the accuracy of numerical methods for solving three-body Coulomb problems since high precision variational calculations are available for comparison.

7.1 Hydrogen atom on a three-dimensional sphere

Consider the following eigenvalue problem

$$\begin{gathered}(-\frac{1}{2\sin^2\alpha}\frac{d}{d\alpha}\sin^2\alpha\frac{d}{d\alpha} - \frac{1}{\mathcal{R}}\cot\alpha)\psi(\alpha;\mathcal{R}) = E(\mathcal{R})\psi(\alpha;\mathcal{R}), \\ \lim_{\alpha\to 0}\sin^2\alpha\frac{\partial\psi}{\partial\alpha} = 0, \qquad \lim_{\alpha\to\pi}\sin^2\alpha\frac{\partial\psi}{\partial\alpha} = 0.\end{gathered} \tag{20}$$

To preserve the form of operators used in previous Sections, we rewrite equation (20) as

$$\left(-\mathcal{R}\frac{d}{d\alpha}\sin^2\alpha\frac{d}{d\alpha} - \mathcal{R}^2\sin 2\alpha\right)\psi(\alpha;\mathcal{R}) = E(\mathcal{R})2\mathcal{R}^3\sin^2\alpha\psi(\alpha;\mathcal{R}).$$

Problem (20) has an analytical solution

$$E_n(\mathcal{R}) = -\frac{1}{2}\left[\frac{1}{n^2} - \frac{n^2-1}{\mathcal{R}^2}\right], \quad n = 1, 2, \ldots$$

with eigenfunctions $\psi_n(\alpha;\mathcal{R})$ which are the radial functions of a hydrogen atom on a three-dimensional sphere [18, 19]

$$\psi_n(\alpha,\mathcal{R}) = C_n(\mathcal{R})Re\{\exp[-\imath\alpha(n-1-\imath\sigma)]_2F_1(-n+1, 1+\imath\sigma, 2, 1-\exp(2\imath\alpha))\},$$

$$C_n(\mathcal{R}) = \frac{2}{\sqrt{1-\exp(-2\pi\sigma)}}\sqrt{\sigma\frac{n^2+\sigma^2}{\mathcal{R}^3}}, \quad \sigma = \frac{\mathcal{R}}{n},$$

where ${}_2F_1$ is a full hypergeometric function.

Denote the exact solutions of problem (20) by (E_n, ψ_n) and the numerical ones by (E_n^h, ψ_n^h). First, we present the results of the computation of eigenvalues and their derivatives, which were obtained using 100 finite elements of the fifth order (501 nodes). Twenty eigenvalues were calculated simultaneously at two values of hyperradius $\mathcal{R} = 1$ and 15 a.u. Some of them are presented in Tables 1 and 2 together with quantities $\epsilon = E_n^h - E_n$ and $\delta = (E_n^h)' - E_n'$ which show the actual accuracy achieved for the approximate eigenvalues and their derivatives. From the Tables, one can see an excellent agreement (10^{-10} or better) of our numerical results with the exact solutions.

In order to compare the accuracy of radial matrix elements computed from the analytical and numerical solutions, we denote matrices $\mathbf{Q}$ and $\mathbf{H}$ calculated using exact solutions (E_n, ψ_n) with the help of expressions (8) and (14)-(15) by $\mathbf{Q^1}$, $\mathbf{H^1}$ and $\mathbf{Q^2}$, $\mathbf{H^2}$, respectively, and the ones calculated from (E_n^h, ψ_n^h) by $\mathbf{Q^{1h}}$, $\mathbf{H^{1h}}$ and $\mathbf{Q^{2h}}$, $\mathbf{H^{2h}}$, respectively. To simplify the comparison between the analytical and numerical solutions we introduce the following quantities

$$q_1 = \max_{1\le i,j\le 20}|Q_{ij}^1 - Q_{ij}^{1h}|, \quad q_2 = \max_{1\le i,j\le 20}|Q_{ij}^2 - Q_{ij}^{2h}|, \quad q_3 = \max_{1\le i,j\le 20}|Q_{ij}^{1h} - Q_{ij}^{2h}|,$$

$$h_1 = \max_{1\le i,j\le 20}|H_{ij}^1 - H_{ij}^{1h}|, \quad h_2 = \max_{1\le i,j\le 20}|H_{ij}^2 - H_{ij}^{2h}|, \quad h_3 = \max_{1\le i,j\le 20}|H_{ij}^{1h} - H_{ij}^{2h}|.$$

In Table 3, we compare the results of our computations with the analytical solutions obtained for $\mathcal{R} = 1$ and 15 a.u. One can see that radial matrix elements calculated within the present approach agree very well (10^{-8} or better) with the exact ones for given values of $\mathcal{R}$. Note that our numerical results are also in an excellent agreement with theoretical estimates (13).

Consider next the convergence of formula (15) with respect to the size of the adiabatic basis set (number of parametric eigenvalues $E_i(\mathcal{R})$). In order to do that we have calculated the following constructs

$$H_{ij}^{2h,m} = -\sum_{l}^{m} Q_{il}Q_{lj}, \quad 1 \le i,j \le m, \quad m = 1, 2, \ldots, 20.$$

Table 1: Approximate eigenvalues E_n^h of problem (20) and their derivatives $(E_n^h)'$ calculated at $\mathcal{R} = 1$ a.u. The accuracy of the E_n^h and $(E_n^h)'$ with respect to the exact solutions is presented by quantities $\epsilon = E_n^h - E_n$ and $\delta = (E_n^h)' - E_n'$. 100 finite elements of the fifth order (501 nodes) have been used. The number in parentheses denote power of ten.

n	E_n^h	ϵ	$(E_n^h)'$	δ
1	−.4999999999(+00)	.266(−11)	−.5748734821(−11)	.575(−11)
2	.1375000000(+01)	.253(−11)	−.3000000000(+01)	−.264(−11)
3	.3944444444(+01)	.986(−12)	−.8000000000(+01)	−.101(−11)
4	.7468750000(+01)	.476(−12)	−.1500000000(+02)	−.490(−12)
5	.1198000000(+02)	.125(−12)	−.2400000000(+02)	−.111(−12)
6	.1748611111(+02)	.137(−12)	−.3500000000(+02)	−.154(−12)
8	.3149218750(+02)	.122(−13)	−.6300000000(+02)	−.246(−13)
10	.4949499999(+02)	.301(−13)	−.9900000000(+02)	−.144(−14)
12	.7149652777(+02)	.793(−13)	−.1429999999(+03)	−.761(−13)
14	.9749744897(+02)	.114(−12)	−.1949999999(+03)	−.108(−12)
16	.1274980468(+03)	.105(−12)	−.2549999999(+03)	−.100(−12)
18	.1614984567(+03)	.310(−13)	−.3229999999(+03)	−.191(−12)
20	.1994987500(+03)	.464(−12)	−.3990000000(+03)	−.107(−09)

Table 2: Approximate eigenvalues E_n^h of problem (20) and their derivatives $(E_n^h)'$ calculated at $\mathcal{R} = 15$ a.u. The accuracy of the E_n^h and $(E_n^h)'$ with respect to the exact solutions is shown by quantities $\epsilon = E_n^h - E_n$ and $\delta = (E_n^h)' - E_n'$. 100 finite elements of the fifth order (501 nodes) have been used. The number in parentheses denote power of ten.

n	E_n^h	ϵ	$(E_n^h)'$	δ
1	−.4999999999(+00)	.857(−11)	.6063205493(−12)	.606(−12)
2	−.1183333333(+00)	.353(−11)	−.8888888888(−03)	−.600(−10)
3	−.3777777777(−01)	.377(−11)	−.2370370370(−02)	−.689(−11)
4	.2083333333(−02)	.431(−10)	−.4444444444(−02)	−.179(−11)
5	.3333333333(−01)	.261(−11)	−.7111111111(−02)	−.113(−12)
6	.6388888888(−01)	.144(−11)	−.1037037037(−01)	−.555(−12)
8	.1321875000(+00)	.761(−12)	−.1866666666(−01)	−.305(−13)
10	.2150000000(+00)	.496(−12)	−.2933333333(−01)	−.459(−12)
12	.3143055555(+00)	.352(−12)	−.4237037037(−01)	−.938(−13)
14	.4307823129(+00)	.252(−12)	−.5777777777(−01)	−.294(−12)
16	.5647135416(+00)	.247(−12)	−.7555555555(−01)	−.125(−12)
18	.7162345679(+00)	.363(−12)	−.9570370370(−01)	−.173(−12)
20	.8854166666(+00)	.823(−12)	−.1182222222(+00)	−.782(−10)

Table 3: Comparison between analytical and numerical matrix elements calculated using exact solutions (E_n, ψ_n) and the approximate ones, (E_n^h, ψ_n^h). Quantities q_1, q_2, q_3, h_1, and h_2 are defined in the text. The numerical scheme parameters are the same as in Table 1.

$\mathcal{R}$	q_1	q_2	q_3	h_1	h_2
$\mathcal{R} = 1$	.308(−08)	.593(−11)	.732(−11)	.381(−08)	.461(−08)
$\mathcal{R} = 15$	.663(−08)	.178(−14)	.696(−13)	.787(−08)	.817(−08)

Table 4: Convergence of the h_3^m as a function of the number of the adiabatic eigensolutions m ($m = 5, 10, 15, 20$). h_3^m is defined in the text. The numerical scheme parameters are the same as in Table 1.

$\mathcal{R}$	h_3^5	h_3^{10}	h_3^{15}	h_3^{20}
$\mathcal{R} = 1$	.473(−06)	.342(−05)	.133(−04)	.162(−02)
$\mathcal{R} = 15$	.195(−04)	.195(−04)	.195(−04)	.127(−02)

Table 5: Eigenvalues (adiabatic potential curves) $E_i(\mathcal{R})$ and their derivatives $dE_i(\mathcal{R})/d\mathcal{R}$, $i = 1, \ldots, 6$, of problem (11) computed at $\mathcal{R} = 7.65$ a.u. The results of the calculations of the E_i^h and $(E_i^h)'$ performed by the present method are presented in the second and fifth columns, respectively. Seven differential equations (11) ($l_{\max} = 6$) have been solved using 68 finite elements of the seventh order (477 nodes). For comparison, the results of the computations of the $\tilde{E}_i^h$ and $\overline{E}_i^h$ for two different sets of numerical parameters carried out by the method of Ref. [21] are given in the third and fourth columns, respectively. The $\tilde{E}_i^h$ have been computed in [21] using 68 finite elements of the seventh order with $l_{\max} = 6$ and $k_{\max} = 8$ ($l_{\max}$ and $k_{\max}$ are defined in the text). The $\overline{E}_i^h$, $i = 1, \ldots, 80$, have been obtained using the same number and order of finite elements with $l_{\max} = 6$ and $k_{\max} = 15$ (only the first 6 eigenvalues are displayed).

i	E_i^h	$\tilde{E}_i^h$	$\overline{E}_i^h$	$(E_i^h)'$
1	−2.13590169	-2.1358893	-2.1358894	.18574453(−01)
2	−.698907137	-.69893960	-.69893964	.46093945(−01)
3	−.617951769	-.61794757	-.61794766	.19973460(−01)
4	−.422639095	-.42279391	-.42279421	−.22691387(−01)
5	−.371634497	-.37170963	-.37171011	−.16109094(−01)
6	−.269808873	-.26968352	-.26968483	−.21915412(−01)

The results for the h_3^m calculated from the H_{ij}^{1h} and $H_{ij}^{2h,m}$ for some values of m are shown in Table 4. From the Table, one can see that matrix elements $H_{ij}^{2h,m}$ calculated using formula (15) show poor convergence in m and therefore lower accuracy and computational efficiency in comparison with the ones obtained from Eqs. (8). This result is important in the context of the next subsection since in order to get the desired level of accuracy of solutions of three-body problem within the adiabatic representation we need to calculate potential matrices $\mathbf{Q}(\mathcal{R})$ and $\mathbf{V}(\mathcal{R})$ with the same accuracy as surface functions $\Phi_i(\alpha,\theta;\mathcal{R})$. The fulfillment of this requirement is guaranteed in the proposed approach.

7.2 Helium atom and negative hydrogen ion

In this subsection we present numerical results of solving problem (1)-(3) for the ground state of the helium atom and negative hydrogen ion. First, let us examine the accuracy of the potential curves $E_i(\mathcal{R})$ and potential matrix elements $Q_{ij}(\mathcal{R})$ and $H_{ij}(\mathcal{R})$ within the present method for the helium atom. These calculations can be directly compared with the results of calculations for the helium atom performed in Refs. [20, 21] using another implementation of the adiabatic hyperspherical approach. In [20, 21], a different numerical method for constructing the adiabatic functions $\Phi_i(\alpha,\theta;\mathcal{R})$ has been used. Matrix elements $Q_{ij}(\mathcal{R})$ were calculated in [20, 21] as

$$Q_{ij}(\mathcal{R}) = [\mathcal{R}^2(E_i(\mathcal{R}) - E_j(\mathcal{R}))]^{-1}\langle\Phi_i(\alpha,\theta;\mathcal{R})|\hat{W}(\alpha,\theta)|\Phi_j(\alpha,\theta;\mathcal{R})\rangle \qquad (21)$$

and $H_{ij}(\mathcal{R})$ were obtained by Eq. (15). In order to compare our results with the ones reported in [21], we have calculated potential curves $E_i(\mathcal{R})$, $i = 1,\ldots,6$, and potential matrix elements $Q_{ij}(\mathcal{R})$ and $H_{ij}(\mathcal{R})$, $i,j = 1,\ldots,6$, at fixed value of hyperradius $\mathcal{R} = 7.65$ a.u. For solving Eq. (11) consisting of seven equations ($l_{\max} = 6$), 68 finite elements of the seventh order (477 nodes) have been used. Our results for the $E_i(\mathcal{R} = 7.65)$ and $Q_{ij}^{1h}(\mathcal{R} = 7.65)$ agree very well with the $Q_{ij}^{2h}(\mathcal{R} = 7.65)$ obtained by Eq. (21) in [21] with the same number and order of finite elements (477 grid points), $l_{\max} = 6$ and $k_{\max} = 8$ ($k_{\max}$ here is the number of eigenvalues of auxiliary one-dimensional adiabatic Hamiltonian [21]). However, some of our matrix elements $H_{ij}^{1h}(\mathcal{R} = 7.65)$ differ significantly (up to the factor 1.7) from the $H_{ij}^{2h}(\mathcal{R} = 7.65)$ elements obtained in [21]. Analysis of these results (presented below in Table 7) has showed that in order to get a better agreement between the two methods for the $H_{ij}(\mathcal{R})$, it is necessary to increase the value of $k_{\max}$ from 8 up to 15 and also increase the number of terms in sum (15) from 6 up to 80. Only using this

extended basis set matrix elements $H_{ij}^{2h}(\mathcal{R} = 7.65)$ calculated by the method of Ref. [21] could approach the ones obtained by using Eq. (8).

In Table 5 we present the results of our calculations of potential curves E_i^h and their derivatives $(E_i^h)'$, $i = 1,\ldots,6$, with accuracy 10^{-10} a.u. at $\mathcal{R} = 7.65$ a.u. These results are compared with the $\tilde{E}_i^h$ (the third column) reported in [21] and the $\overline{E}_i^h$ (the fourth column) calculated using the extended set of numerical parameters described in the paragraph above. There is a very good agreement between these three calculations. However, it is worth to mention, that eigenvalues E_i^h are solutions of Eq. (11) obtained using zero-gradient (Neumann) boundary conditions whereas $\tilde{E}_i^h$ and $\overline{E}_i^h$ have been obtained as solutions of the auxiliary one-dimensional eigenvalue problem (see Eq. (12) of Ref. [21]) using zero-value (Dirichlet) boundary conditions. Also matrix elements V_{ij} are calculated differently (compare Eq. (11) of Ref. [21] and Eq. (11) and formula for V_{ij} below Eq. (11) in the present work), which results in the different rate of convergence of the corresponding angular expansions.

In Table 6 we present our calculations of matrix elements $Q_{ij}^{1h}(\mathcal{R} = 7.65)$ and $Q_{ij}^{2h}(\mathcal{R} = 7.65)$ obtained by formulas (8) and (14), respectively. The results of both calculations are practically identical within the given accuracy. For comparison, we show in Table 6 matrix elements $\tilde{Q}_{ij}^{2h}(\mathcal{R} = 7.65)$ (the fifth column) obtained by formula (21) in [21] and also $\overline{Q}_{ij}^{2h}(\mathcal{R} = 7.65)$ (the sixth column) calculated by the same method but using the extended basis set described above. One can see a very good agreement between all four calculations presented in the Table.

In Table 7 we present our results for radial matrix elements $H_{ij}^{1h}(\mathcal{R} = 7.65)$ and $H_{ij}^{2h}(\mathcal{R} = 7.65)$ obtained within the present approach using formulas (8) and (15), respectively. The results for the $H_{ij}^{2h}(\mathcal{R} = 7.65)$ have been obtained using six terms in sum (15). One can easily see a big difference between these two calculations. A similar discrepancy is observed between the $H_{ij}^{1h}(\mathcal{R} = 7.65)$ and the $\tilde{H}_{ij}^{2h}(\mathcal{R} = 7.65)$ (the fifth column in Table 7) taken from Ref. [21]. As one could expect, our $H_{ij}^{2h}(\mathcal{R} = 7.65)$ elements agree much better with the $\tilde{H}_{ij}^{2h}(\mathcal{R} = 7.65)$ obtained with the same number of terms in formula (15). Such disagreement between the H_{ij}^{1h} and the H_{ij}^{2h} and $\tilde{H}_{ij}^{2h}$ is because of insufficient number of terms (six only) taken into account in sum (15) for the H_{ij}^{2h} and $\tilde{H}_{ij}^{2h}$. In order to show that matrix elements H_{ij}^{1h} are much more accurate than the H_{ij}^{2h} and $\tilde{H}_{ij}^{2h}$ ones, we have calculated the $\overline{H}_{ij}^{2h}$ (see the sixth column in Table 7) using 80 terms in sum (15). Comparison of the third and

Table 6: Matrix elements of radial coupling $Q_{ij}(\mathcal{R})$ computed at $\mathcal{R} = 7.65$ a.u. The results of the present calculation of the Q_{ij}^{1h} and Q_{ij}^{2h} obtained by using formulas (8) and (14) are presented in the third and fourth columns, respectively. The results of the calculation of the $\tilde{Q}_{ij}^{2h}$ and $\overline{Q}_{ij}^{2h}$ by the method of Ref. [21] using formula (21) for two different sets of numerical parameters are given in the fifth and sixth columns, respectively. The numerical scheme parameters are the same as in Table 5. The number in parentheses denote power of ten.

i	j	Q_{ij}^{1h}	Q_{ij}^{2h}	$\tilde{Q}_{ij}^{2h}$	$\overline{Q}_{ij}^{2h}$
1	2	.586014(−01)	.586014(−01)	.585907(−01)	.585893(−01)
1	3	−.286341(−01)	−.286341(−01)	.286413(−01)	.286418(−01)
1	4	.442209(−01)	.442209(−01)	.442198(−01)	.442216(−01)
1	5	−.336214(−01)	−.336214(−01)	.336215(−01)	.336233(−01)
1	6	.161869(−01)	.161869(−01)	.162012(−01)	.162002(−01)
2	3	.250621(−01)	.250621(−01)	−.250045(−01)	−.250077(−01)
2	4	.165765(+00)	.165765(+00)	.165781(+00)	.165782(+00)
2	5	−.607837(−01)	−.607837(−01)	.607890(−01)	.607908(−01)
2	6	.172490(−01)	.172490(−01)	.172592(−01)	.172573(−01)
3	4	.457925(−01)	.457925(−01)	−.458364(−01)	−.458311(−01)
3	5	.134640(+00)	.134640(+00)	.134615(+00)	.134617(+00)
3	6	−.896893(−01)	−.896893(−01)	.897034(−01)	.897034(−01)
4	5	−.203183(+00)	−.203183(+00)	.202920(+00)	.202961(+00)
4	6	.155380(−01)	.155380(−01)	.155163(−01)	.155172(−01)
5	6	−.113957(+00)	−.113957(+00)	.113800(+00)	.113799(+00)

Table 7: Matrix elements of radial coupling $H_{ij}(\mathcal{R})$ computed at $\mathcal{R} = 7.65$ a.u. The results of the present calculation of the H_{ij}^{1h} and H_{ij}^{2h} obtained by using formulas (8) and (15) are presented in the third and fourth columns, respectively. The results of the calculation of the $\tilde{H}_{ij}^{2h}$ and $\overline{H}_{ij}^{2h}$ by the method of Ref. [21] using formula (15) for two different sets of numerical parameters are given in the fifth and sixth columns, respectively. The numerical scheme parameters are the same as in Table 5. The number in parentheses denote power of ten.

i	j	H_{ij}^{1h}	H_{ij}^{2h}	$\tilde{H}_{ij}^{2h}$	$\overline{H}_{ij}^{2h}$
1	1	.129180(−01)	.760195(−02)	.760548(−02)	.128801(−01)
1	2	.126385(−01)	.893549(−02)	.947869(−02)	.126303(−01)
1	3	−.729629(−02)	−.542228(−02)	.648605(−02)	.728683(−02)
1	4	.376942(−02)	−.132001(−02)	−.129332(−02)	.375300(−02)
1	5	−.105365(−01)	.145577(−01)	−.145408(−01)	−.105361(−01)
1	6	−.599567(−02)	−.809748(−02)	−.825414(−02)	−.599308(−02)
2	2	.387063(−01)	.355324(−01)	.372254(−01)	.387056(−01)
2	3	−.450057(−02)	−.381820(−02)	.593952(−02)	.449231(−02)
2	4	.190126(−01)	.140620(−01)	.244742(−01)	.189969(−01)
2	5	.238220(−01)	.263704(−01)	−.156242(−01)	−.238009(−01)
2	6	−.538306(−02)	−.630598(−02)	−.799195(−02)	−.537534(−02)
3	3	.326976(−01)	.297171(−01)	.731349(−01)	.326953(−01)
3	4	−.256900(−01)	−.258621(−01)	.251212(−02)	.256612(−01)
3	5	.226722(−01)	.189643(−01)	−.677882(−02)	.226588(−01)
3	6	.119753(−01)	.146004(−01)	−.185494(−01)	−.119490(−01)
4	4	.814621(−01)	.730553(−01)	−.374142(+00)	.813717(−01)
4	5	−.966072(−02)	−.716772(−02)	−.307431(+00)	.965263(−02)
4	6	−.231241(−01)	−.236861(−01)	.370903(+00)	−.230691(−01)
5	5	.834146(−01)	.772227(−01)	.264643(+00)	.832770(−01)
5	6	−.194731(−01)	−.168255(−01)	.402133(−01)	.194682(−01)
6	6	.273542(−01)	.218313(−01)	−.499955(−02)	.273217(−01)

sixth columns in Table 7 clearly indicates that the $\overline{H}_{ij}^{2h}$ computed with the extended basis set parameters agree much better with the H_{ij}^{1h} obtained by Eq. (8) than with the H_{ij}^{2h} and $\tilde{H}_{ij}^{2h}$ computed by Eq. (15). This confirms our conclusion about the higher accuracy and efficiency of formulas (8) and the necessity to use a rather large number of terms in Eq. (15) (and therefore excessive computational resources) in order to get a comparable accuracy of matrix elements H_{ij}^{2h}. In all our calculations presented below matrix elements Q_{ij} and H_{ij} are calculated using formulae (8).

In order to study the convergence of potential curves $E_i(\mathcal{R})$ and radial matrix elements $Q_{ij}(\mathcal{R})$ and $H_{ij}(\mathcal{R})$ we have performed a set of computations of these quantities as functions of numerical scheme parameters, namely, number of isoparametric Lagrange elements $N_{\rm el}$, their order $N_{\rm pol}$ and maximum number of terms $l_{\rm max}$ in the angular basis set expansion in l (see Eq. (9). The results of some of these calculations for the E_i, E_j, Q_{ij}, H_{ij} and H_{jj}, $i = 3$, $j = 5$, computed at $\mathcal{R} = 7.65$ a.u. are presented in Table 8. In the present work, the desired accuracy of the ground state energy of He and H^- is set to 10^{-6} a.u. This requires the same accuracy of radial matrix elements, as well. From Table 8, the following set of numerical parameters has been chosen for the He $^1S^e$ state: $N_{\rm el} = 210$ (1471 grid points with $h = 0.00053$), $N_{\rm pol} = 7$, and $l_{\rm max} = 11$ (12 equations in Eq. (11)). The grid in $\mathcal{R}$ has been chosen as follows, 0.02(0.02)0.32(0.01)1(0.02)3(0.05)5(0.08)9(0.1)20(0.2)30(0.25)50 (number in parentheses denotes the step in $\mathcal{R}$). A banded system of 17652 linear algebraic equations, [Eq. (12)], has been solved with relative error tolerance $\epsilon = 10^{-10}$ at each value of hyperradius $\mathcal{R}$ with the mean half bandwidth MHB = 54 (maximum 96). In Fig. 1 we show the He $^1S^e$ potential curves $E_i(\mathcal{R})$, $i = 1, ..., 28$, correlating with the $n = 1 - n = 7$ hydrogenic-like states of He^+ as a function of hyperradius $\mathcal{R}$. Clearly seen are points of avoided crossings [2, 6] where the radial non-adiabatic coupling terms are known [2, 6, 7] to peak. Such peaks are clearly seen from Fig. 2 where the diagonal matrix elements H_{ii}, $i = 1, 2, 3, 4, 5, 8, 28$, are presented. For instance, matrix elements H_{22} and H_{33} and also H_{44} and H_{55} in Fig. 2 show pronounced maxima in the avoided crossing regions.

In Fig. 3 we plotted radial coupling matrix elements $Q_{ij}(\mathcal{R})$ for some values of i and j as functions of hyperradius $\mathcal{R}$. As can be seen from the Figure, the matrix elements displayed also show maxima in the quasi-crossings points. Note that singular behaviour of the radial matrix elements near avoided crossings can be eliminated by passing into the diabatic representation [22]. However, in this work we use the finite element scheme which

Table 8: Convergence of potential curves E_i, E_j (in a.u.) and matrix elements Q_{ij}, H_{ij} and H_{jj}, $i = 3$, $j = 5$, as functions of maximum number ot terms $l_{\rm max}$ in expansion (9), number of finite elements $N_{\rm el}$ and their order $N_{\rm pol}$ evaluated at $\mathcal{R} = 7.65$ a.u.

$l_{\rm max}$	$N_{\rm el}$	$N_{\rm pol}$	E_3	E_5	Q_{35}	H_{35}	H_{55}
5	68	7	−.6179400	−.3716334	.134666	.022636	.083357
6	68	7	−.6179518	−.3716345	.134640	.022672	.083415
7	68	7	−.6179578	−.3716348	.134630	.022690	.083444
8	68	7	−.6179611	−.3716348	.134626	.022700	.083460
9	68	7	−.6179632	−.3716349	.134624	.022705	.083470
10	68	7	−.6179645	−.3716349	.134622	.022709	.083477
11	68	7	−.6179654	−.3716349	.134622	.022712	.083481
12	68	7	−.6179660	−.3716349	.134621	.022713	.083484
13	68	7	−.6179664	−.3716349	.134621	.022714	.083486
14	68	7	−.6179667	−.3716349	.134621	.022715	.083487
6	68	4	−.6179550	−.3715759	.134659	.022683	.083528
6	68	5	−.6179539	−.3715960	.134652	.022679	.083489
6	68	6	−.6179523	−.3716254	.134643	.022674	.083432
6	68	7	−.6179518	−.3716345	.134640	.022672	.083415
6	40	7	−.6179546	−.3715826	.134656	.022682	.083515
6	80	7	−.6179512	−.3716456	.134637	.022670	.083393
6	120	7	−.6179500	−.3716667	.134630	.022666	.083353
6	160	7	−.6179494	−.3716772	.134627	.022664	.083333
6	200	7	−.6179491	−.3716836	.134625	.022663	.083321
6	240	7	−.6179489	−.3716878	.134624	.022663	.083313

Table 9: Comparison of the numerical potential curves $E_i(\mathcal{R})$ with the dipole asymptotics, $E_i^{\rm as}(\mathcal{R})$, for the ^{1}S^e state of He calculated at $\mathcal{R} = 40$, 60 and 80 a.u. up to the $n = 3$ threshold.

Curve	$\mathcal{R} = 40$ a.u.		$\mathcal{R} = 60$ a.u.		$\mathcal{R} = 80$ a.u.	
number, i	$-E_i(\mathcal{R})$	$-E_i^{\rm as}(\mathcal{R})$	$-E_i(\mathcal{R})$	$-E_i^{\rm as}(\mathcal{R})$	$-E_i(\mathcal{R})$	$-E_i^{\rm as}(\mathcal{R})$
1	2.02516	2.02516	2.01674	2.01674	2.01254	2.01254
2	0.52627	0.52620	0.51722	0.51720	0.51281	0.51280
3	0.52413	0.52411	0.51628	0.51627	0.51228	0.51228
4	0.25103	0.25073	0.24052	0.24045	0.23563	0.23560
5	0.24735	0.24693	0.23888	0.23876	0.23470	0.23465
6	0.24437	0.24447	0.23765	0.23766	0.23403	0.23403

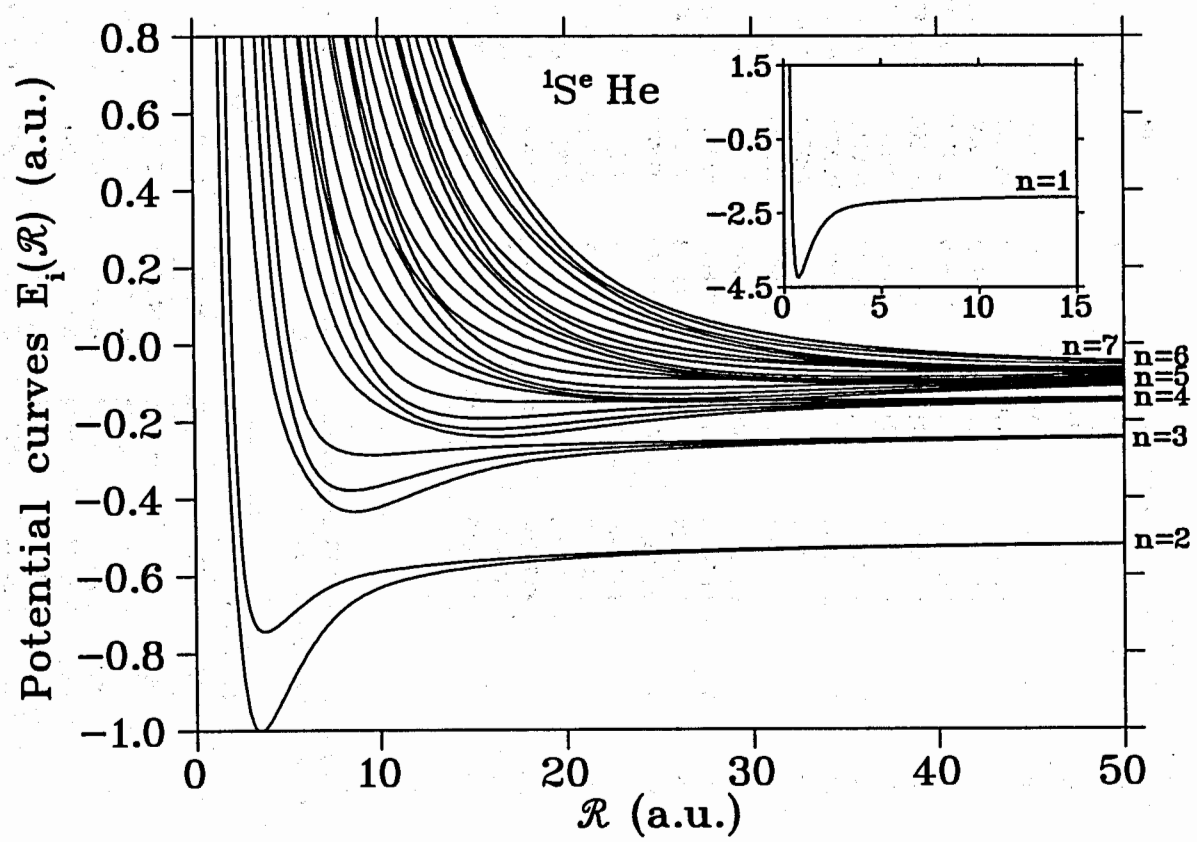

Figure 1: Potential curves $E_i(\mathcal{R})$ (in a.u.) plotted vs hyperradius $\mathcal{R}$ up to the $n = 7$ threshold for the $^1S^e$ state of He.

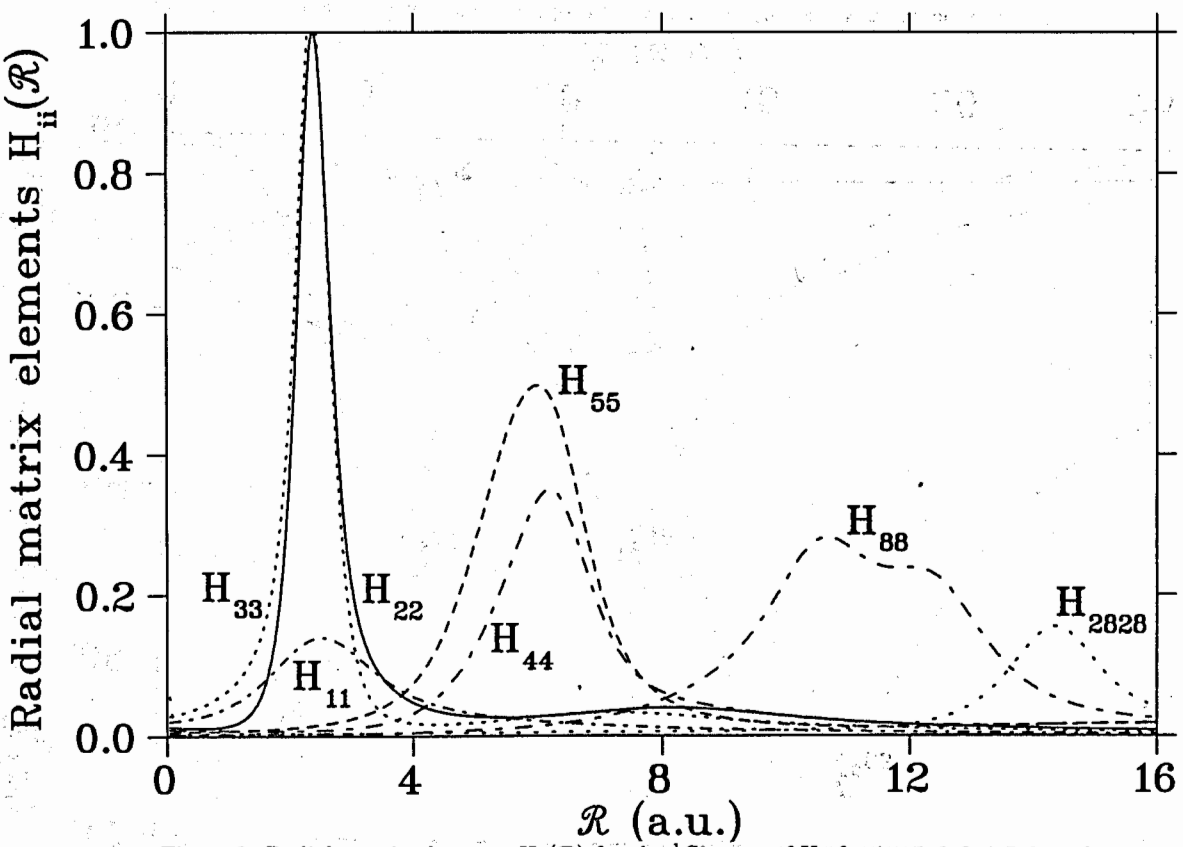

Figure 2: Radial matrix elements $H_{ii}(\mathcal{R})$ for the $^1S^e$ state of He for $i = 1, 2, 3, 4, 5, 8$, and 28.

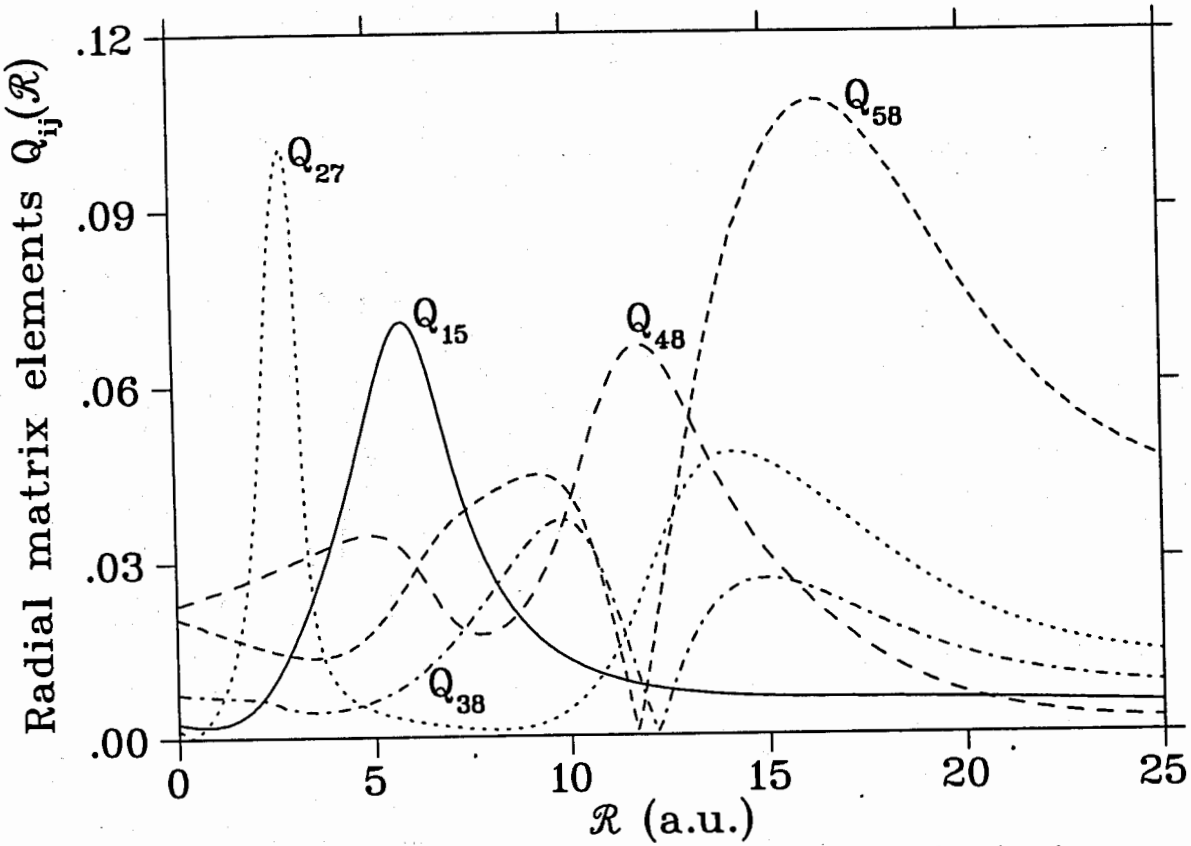

Figure 3: Radial matrix elements $Q_{ij}(\mathcal{R})$ for the $^1S^e$ state of He for several values of i and j.

allows us to solve the eigenvalue problem for system of radial eauations (6) within the adiabatic representation.

In Table 9 we compare potential curves $E_i(\mathcal{R})$ calculated numerically with the asymptotic ones, $E_i^{as}(\mathcal{R})$, computed analytically using the dipole approximation [23] for three values of $\mathcal{R} = 40$, 60 and 80 a.u. up to the $n = 3$ threshold. It is evident that these results agree very well. For instance, the five significant digits are obtained for the ground state potential curve ($i = 1$). This confirms the high accuracy of our numerical procedure.

For H^- the following set of numerical parameters has been chosen: $N_{el} = 220$ (1541 grid points with $h = 0.00051$), $N_{pol} = 7$, $l_{max} = 11$, $\epsilon = 10^{-10}$, and the $\mathcal{R}$ region has been divided as follows, 0.02(0.08)0.98(0.02)1(0.025)3(0.05)5(0.075)7.1(0.1)20(0.2)30(0.25)50. The size of a banded system of linear algebraic equations, [Eq. (12)], was 18492 with the mean half bandwidth MHB = 54 (maximum 99). In Fig. 4 the H^- $^1S^e$ potential curves $E_i(\mathcal{R})$, $i = 1, ..., 28$, up to the $n = 7$ hydrogenic threshold are shown as functions of hyperradius $\mathcal{R}$. From the Figure, one can see a lot of quasi-crossing points, as well as several exact crossings.

The system of coupled radial equations (6) has been solved subject to boundary conditions (7) by the finite element method using schemes of high-order accuracy [16, 17]. Isoparametric Lagrange elements of the third order have been used which provide an accuracy of $O(h_{\mathcal{R}}^6)$ order with respect to eigenvalues and of $O(h_{\mathcal{R}}^4)$ order with respect to eigenfunctions. Here $h_{\mathcal{R}}$ is the maximum mesh step of the finite-element grid on the interval $[0, \mathcal{R}_{max}]$. As a result of numerical experiments, the following values of numerical scheme parameters have been chosen: (i) $\mathcal{R}_{max} = 40$ a.u. and $N_{el} = 1500$ (4501 grid points with step $h_{\mathcal{R}} = 0.0089$) for the He atom; and (ii) $\mathcal{R}_{max} = 30$ a.u. and $N_{el} = 1200$ (3601 grid points with $h_{\mathcal{R}} = 0.0082$) for the H^- ion. The size of a banded system of linear algebraic equations, [Eq. (12)], approximated a system of 28 radial equations was 125972 with MHB = 70 (maximum 112) for the He and 100772 with MHB = 70 (maximum 112) for the H^-, respectively. Error tolerance has been set to 10^{-12} a.u.

A convergence study of the ground state energy of He and H^- with the number of radial equations is presented in Table 10. One can see that the energy eigenvalues converge monotonically from above, with the 28-channel value being $E_{He} = -2.90372266$ a.u. and $E_{H^-} = -0.52774970$ a.u. As shown in Table 11, these values are very close to the precision variational results [26]: $E_{He}^{VAR} = -2.90372437$ a.u. and $E_{H^-}^{VAR} = -0.52775102$ a.u. Since the

Table 10: Convergence of the ground state energy (in a.u.) for He and H^- with the number of coupled channels n.

n	He	H^-
1	−2.88791168	−0.52241442
2	−2.89137991	−0.52472087
3	−2.90287002	−0.52732522
6	−2.90300448	−0.52751473
10	−2.90363613	−0.52768020
15	−2.90370549	−0.52773607
21	−2.90372264	−0.52774928
28	−2.90372266	−0.52774970

Table 11: Comparison of the present ground state energy (in a.u.) of He and H^- with other theoretical calculations.

Method	He	H^-
HACC[a]	−2.903723	−0.527750
ACM[b]	−2.903611	−0.527642
HSCC[c]	−2.903594	−0.52773
VAR[d]	−2.903724	−0.527751
MCHF[e]	−2.902909	−0.527542
CI[f]	−2.90323	−0.527542
RMM[g]	−2.8961	−0.52403
CCM[h]	−2.8934	−0.52775

[a] Present 28–channel hyperspherical adiabatic coupled-channel calculation

[b] 17–channel hyperspherical artificial channel method calculation [20]

[c] Hyperspherical close–coupling calculation: 28–channel computation for H^- [24] and 21–channel calculation for He [25]

[d] Variational method calculation [26]

[e] Multiconfigurational Hartree–Fock calculation: using 32 configurations for H^- [27] and 10 configurations for He [28]

[f] Configuration interaction method calculation: using 130 configurations for H^- [29] and He [30]

[g] R–matrix method calculation: using 158 configurations for H^- [31] and 79 configurations for He [32]

[h] Close–coupling method calculation with pseudostates and correlation terms: nine Hylleraas–type functions for H^- [33] and seven correlation functions for He [34]

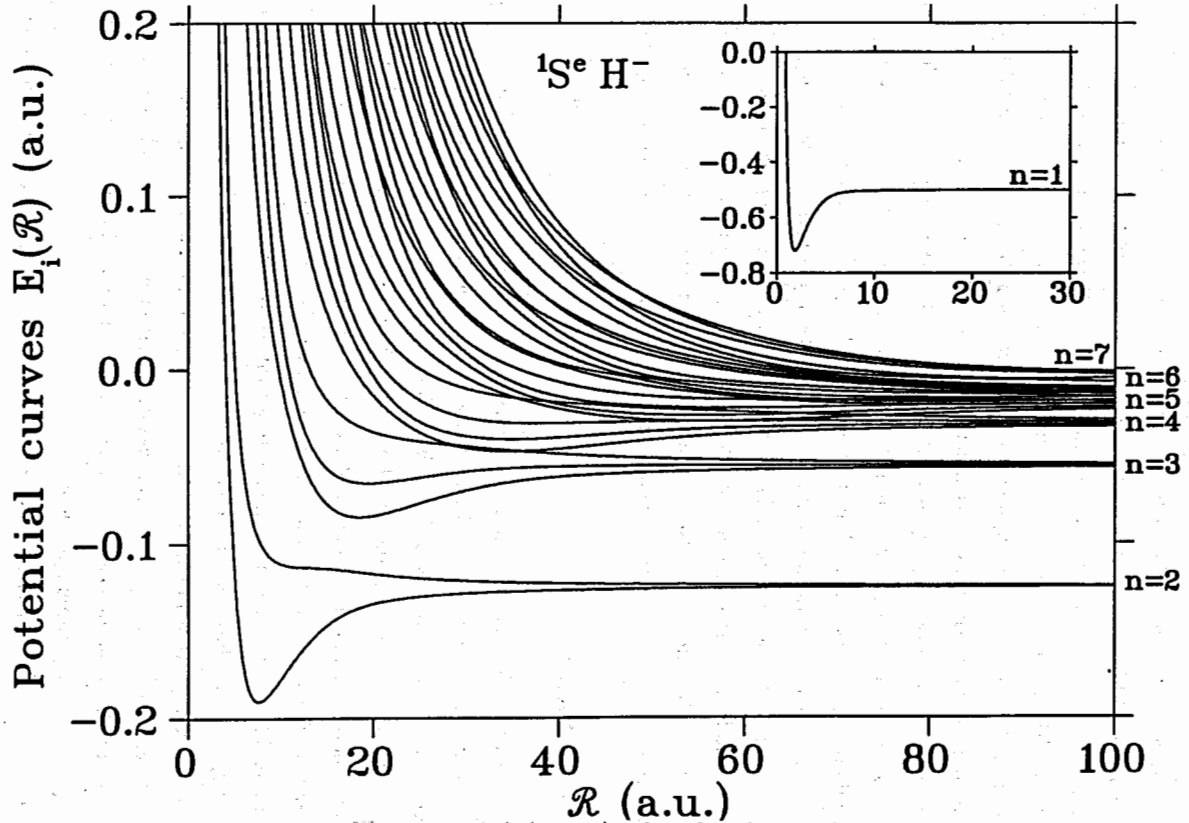

Figure 4: Potential curves $E_i(\mathcal{R})$ (in a.u.) plotted vs hyperradius $\mathcal{R}$ up to the $n = 7$ threshold for the $^1S^e$ state of H^-.

calculation accuracy for eigenvalues equals $O(h_\rho^6)$ and the basis step of the grid amounts to ≈ 0.009, our results have errors in the 12th digit. However, as follows from Table 11, our energy values lie above the variational energies by approximately 10^{-6} a.u. This is consistent with the accuracy of the radial matrix elements and used approximations. Comparison with some other calculations are also given in Table 11. It is evident that our results are more accurate than the 17-channel hyperspherical artificial channel method [20] and the hyperspherical close-coupling method [24, 25]. Both of these methods use the sector-diabatic representation in which adiabatic basis expansion has a slower convergence than in the adiabatic representation used in the present work. We also compare our calculations with the results of the multiconfigurational Hartree–Fock method [27, 28], configuration interaction method [29, 30], R–matrix method [31, 32], and close–coupling method [33, 34]. All these methods use a large number of electronic configurations as seen from Table 11. Analysis of the Table shows that our ground state energies are as accurate or superior to the results of most *ab initio* methods widely used in atomic and molecular calculations.

8 Conclusions

In the present work, the quantum mechanical three-body problem with Coulomb interaction has been formulated within the adiabatic representation method using the hyperspherical coordinates. The reduction of the three-dimensional problem to the one-dimensional one has been performed using the Kantorovich method. A new method for computing variable coefficients (potential matrix elements of radial coupling) of a final system of ordinary second-order differential equations has been proposed. In this method, a new boundary parametric problem with respect to unknown derivatives of eigensolutions in the adiabatic variable (hyperradius) has been formulated. An efficient, fast and stable algorithm for solving the boundary problem with the same accuracy for the adiabatic eigenfunctions and their derivatives has been suggested. As a result, matrix elements of radial coupling can be calculated with the same precision as the adiabatic functions obtained as solutions of an auxiliary parametric eigenvalue problem.

The method developed has been thoroughly tested on a parametric eigenvalue problem for a hydrogen atom on a three-dimensional sphere. This problem has an analytical solution which allowed a direct comparison of our results with the exact solutions. An excellent agreement between the analytical and numerical results has been obtained. The accuracy,

efficiency and robustness of the algorithm have been studied for this problem in details. The method has been further applied to the computation of the ground state energy of the helium atom and negative hydrogen ion. The results obtained show an excellent agreement with the results of calculations by other methods.

This study constitutes a major improvement over the standard techniques of the calculation of potential matrix elements of radial coupling within the adiabatic representation method. It guarantees the high accuracy of computing radial matrix elements which is comparable with the accuracy that can be achieved for the adiabatic eigensolutions of the auxiliary parametric eigenproblem. The approach proposed can be easily extended to systems with arbitrary (finite) masses of particles, total angular momentum $J > 0$, and for any appropriate system of coordinates. The method can be also used for atom-diatom reactive scattering and photodissociation. Work on studying spectral characteristics and properties of the exotic atoms [35] within the present approach is currently underway [36].

9 Acknowledgements

The authors express their gratitude to the seminar of Computational Physics of the Laboratory of Computing Techniques and Automation of the JINR and Professor I.V.Puzynin for support and interest to the work. This work was supported in part by project 09-6-0996-93/99 of the JINR, by the RFBR-INTAS under Grant No. 95-0512, by the RFBR under Grant No. 96-02-17715 and Grant No. 98-02-16160, by the Grant of the Bulgarian Committee on the Use of Atomic Energy for Peaceful Purposes and also by the Bulgarian Found of Scientific Investigations under the Grant No. MM - 903.

References

[1] H.F. Mott and H.S. Massey, *Theory of Atomic Collisions*, 3rd. ed. (Oxford Univ. Press, London/New York, 1965).

[2] U. Fano and R.T. Rau, *Atomic Collisions and Spectra* (Wiley, New York, 1986).

[3] *Atomic spectroscopy and collisions using slow antiprotons*, 7-Oct-97, CERN/SPSC 97-19, CERN/SPSC P-307 (1997); *CERN Courier*, **38**, N.8, (1998).

[4] M. Charlton. Prospects for low energy antihydrogen and the ATHENA project, in *Talk at VIII Int. Conf. on Symmetry Methods in Physics, July 28- August 2, 1997* (Dubna, Russia, 1997), *Yad.Fiz.*, **61**, N.11, 1743, (1998).

[5] S.I. Vinitsky and L.I. Ponomarev, *Fiz. Elem. Chastits At. Yadra* **13**, 1336 (1982) [*Sov. J. Part. Nucl.* **13**, 557 (1982)]; L. Bracci and G. Fiorentini, *Phys. Rep.* **86**, 169 (1982).

[6] J. Maček, *J. Phys.* **B1** (1968) 831; U. Fano, *Rep. Progr. Phys.* **46** (1983) 97; C. D. Lin, *Adv. Atom. Mol. Phys.* **22** (1986) 77; C. D. Lin, *Phys. Rep.* **257**, 1 (1995).

[7] A.G. Abrashkevich, M.S. Kaschiev, I.V. Puzynin, and S.I. Vinitsky, *Sov. J. Nucl. Phys.* **48**, 602 (1986).

[8] L.V. Kantorovich and V.I. Krilov. *Approximate Methods of Higher Analysis* (Wiley, New York, 1964) (Gostekhteorizdat, Moscow, 1952).

[9] A. G. Abrashkevich, D. G. Abrashkevich, M. S. Kaschiev, V. Yu. Poida, I.V. Puzynin, and S. I. Vinitsky, *J. Phys. B* **22** (1989) 3957; A. G. Abrashkevich, D. G. Abrashkevich, I. V. Puzynin, and S. I. Vinitsky, *J. Phys. B* **24**, 1615 (1991); A. G. Abrashkevich, D. G. Abrashkevich, M. S. Kaschiev, I. V. Puzynin, and S. I. Vinitsky, *Phys. Rev.* **A45**, 5274 (1992).

[10] J. Botero, *Phys. Rev.* **A35**, 36 (1987); J. Zhou and C.D. Lin, *J. Phys.* **B27**, 5065 (1994).

[11] S. Hara and T. Ishihara, *Phys. Rev.* **A40**, 4232 (1989); N. Fukuda, T. Ishihara, and S. Hara, *Phys. Rev.* **A41**, 145 (1990).

[12] S.I. Vinitsky, V.S. Melezhik, L.I. Ponomarev, I.V. Puzynin, T.P. Puzynina, L.N. Somov, and N.F. Truskova, *Zh. Eksp. Teor. Fiz.* **79**, 698 (1980) [*Sov. Phys. JETP* **52**, 353 (1980)]; I.V. Puzynin and S.I. Vinitsky, *Muon Catalyzed Fusion* **3**, 307 (1988).

[13] L. M. Delves, Nucl. Phys. **9**, 391 (1959); **20**, 275 (1960); F.T. Smith, *Phys. Rev.* **120**, 1058 (1960).

[14] G. Strang and G.J. Fix, *An Analysis of the Finite Element Method* (Prentice Hall, Englewood Cliffs, New York, 1973).

[15] K.J. Bathe, *Finite Element Procedures in Engineering Analysis* (Prentice Hall, Englewood Cliffs, New York, 1982).

[16] A.G. Abrashkevich, D.G. Abrashkevich, M.S. Kaschiev and I.V. Puzynin, *Comput. Phys. Commun.* **85**, 10, 65 (1995).

[17] A.G. Abrashkevich, D.G. Abrashkevich, M.S. Kaschiev, I.V. Puzynin and S.I. Vinitsky, HSEIGV - *A Program for Computing Energy Levels and Radial Wave Functions in the Coupled-Channel Hyperspherical Adiabatic Approach* (JINR Communications No E11-97-335, Dubna, 1997), 27 pp.

[18] A.A. Izmes'tev, *Sov. J. Nucl. Phys.* **52**, 1697 (1990).

[19] S.I. Vinitsky, L.G. Mardoyan, G.S. Pogosyan, A.N. Sissakyan, T.A. Strizh, *Sov. J. Nucl. Phys.* **56**, 61 (1993).

[20] A.G. Abrashkevich and M. Shapiro, *Phys. Rev.* **A50**, 1205 (1994).

[21] A.G. Abrashkevich, D.G. Abrashkevich, and M. Shapiro, *Comput. Phys. Commun.* **90**, 311 (1995).

[22] F. T. Smith, *Phys. Rev.* **179**, 111 (1969).

[23] M. B. Kadomtsev, S.I. Vinitsky, and F. R. Vukajlovich, *Phys. Rev.* **A36**, 4652 (1987); A.G. Abrashkevich, D.G. Abrashkevich, I. V. Puzynin, and S.I. Vinitsky, *J. Phys.* **B24**, 1615 (1991).

[24] J.-Z. Tang, Y. Wakabayashi, M. Matsuzawa, S. Watanabe, and I. Shimamura, Phys. Rev. **A49** (1994) 1021.

[25] J. Z. Tang, S. Watanabe, and M. Matsuzawa, Phys. Rev. **A46**, 2427 (1992).

[26] C. L. Pekeris, Phys. Rev. **126**, 1470 (1962); K. Frankowski and C. Pekeris, *ibid.*, **146**, 46 (1966); **150**, 366(E) (1966).

[27] H. P. Saha, Phys. Rev. **A38**, 4546 (1988).

[28] C. F. Fischer and M. Idrees, J. Phys. B **23**, 679 (1990).

[29] M. Cortés and F. Martín, *ibid.*, **A48**, 1227 (1993).

[30] I. Sánchez and F. Martín, J. Phys. B **23**, 4263 (1990).

[31] H. R. Sadeghpour, C. H. Greene, and M. Cavagnero, Phys. Rev. **A45**, 1587 (1992).

[32] P. Hamacher and J. Hinze, J. Phys. B **22**, 3397 (1989).

[33] A. W. Wishart, J. Phys. B **12**, 3511 (1979).

[34] J. A. Fernley, K. T. Taylor and M. J. Seaton, J. Phys. B **20**, 6457 (1987).

[35] L. G. Mardoyan, I. V. Puzynin, T. P. Puzynina, A. Yu. Tyukhtyev, and S. I. Vinitsky, *Yad.Fiz.*, **61**, N.11, 2104 (1998); [*Physics of Atomic Nuclei*, **61**, N.11, 1997 (1998)].

[36] A.G. Abrashkevich, M.S. Kaschiev and S.I. Vinitsky (work in progress).

Received by Publishing Department
on October 1, 1999.